0488

DAMAGE MECHANISM ANALYSIS OF RC BRIDGE BY NONLINEAR DYNAMIC SIMULATIONS

Limin SUN[1], Yozo GOTO[2], Hidenao HAYASHI[3] And Kenji KOSA[4]

SUMMARY

This paper reports a mechanism analysis of seismic damage to a T-type single column RC bridge. This is a typical viaduct structure employed in Japan, which was seriously damaged during the Hyogoken Nabu (Kobe) Earthquake in 1995. The simulated bridge system includes superstructure, piers, pile foundations and foundation soils. The soil-pile interaction is expressed by springs and dampers evaluated by an equivalent linear finite element method. The input wave of the ground motion is estimated from a record near the site during the Kobe earthquake. The material parameters, including the strengths of concrete, reinforcement and soil, were determined from field investigations and specimen tests. The simulation results showed that: (1) the height of termination of the longitudinal reinforcement significantly affected the strength of the bridge pier. (2) pile damage superstructure eccentricity resulted in larger residual displacement. (3) the effect of bridge pier embedment depth should be taken into account in seismic design, especially when columns are embedded in road pavement. (4) bearing failure may somewhat reduce shear force on the bridge pier. These research results are expected to be helpful in seismic design and in retrofitting similar types of RC bridges.

INTRODUCTION

During the Hyogoken Nanbu Earthquake in 1995, a large number of bridges suffered serious damage, such as yielding of bridge pier, cracking of pile foundations, failure of bearings and unseating of girders (JSCE, 1996 and Priestely, 1996). It is realized that yielding of single column piers is one of the most serious kinds of damage, because it may result in collapse of the whole bridge system. However, even within the same area subjected to similar strong ground motions, some bridges were only slightly damaged. It is conjectured that this was because of differing bridge geometry, strengh of structural elements, soil conditions and so on, as well as the effects of ground motion and interaction of adjacent bridge spans. Therefore, it is necessary to clarify each bridge's damage mechanism.

This paper reports the results of damage mechanism analysis on a reinforced concrete single column bridge pier.

Several factors considered to significantly affect the extent of damage were modeled by nonlinear dynamic simulations. It is hoped that the analysis method used and the results obtained will contribute to the seismic design and retrofitting of bridges.

OUTLINE OF ANALYSIS

Bridge Pier and Soil Condition

The bridge pier for simulation is shown in Fig.1. It is 3.5m in diameter and 12.74m in height. The arrangement of reinforcement bars is also shown. There are 3 layers of longitudinal reinforcement, but the inner layer is terminated 6.45m from the pier bottom. The confinement bars are distributed along the whole height at 30cm

[1] *Technical Research Institute, Obayashi Corporation, Shimokiyoto, Tokyo, Japan Email: lmsun@tri.obayashi.co.jp*
[2] *Technical Research Institute, Obayashi Corporation, Shimokiyoto, Tokyo, Japan*
[3] *Hanshin Expressway Public Corporation, Kyutaro-chou 4-1-3, Chuo-ku, Osaka 541, Japan*
[4] *Hanshin Expressway Public Corporation, Kyutaro-chou 4-1-3, Chuo-ku, Osaka 541, Japan*

spacing. The superstructure is a double-box girder spanning 60m, it weighs 1032ton and is supported by the pier through 8 metal bearings. The pier is supported by 22 piles, each 14.0m long and 1.0m in diameter. The soil conditions are shown in Fig. 2. The ground soil is classified as Class II according to the Design Specifications of Highway Bridges of Japan (JRA, 1996). The material parameters, such as strengths of concrete, reinforcement and soil, were determined from field-investigations and specimen tests after the earthquake.

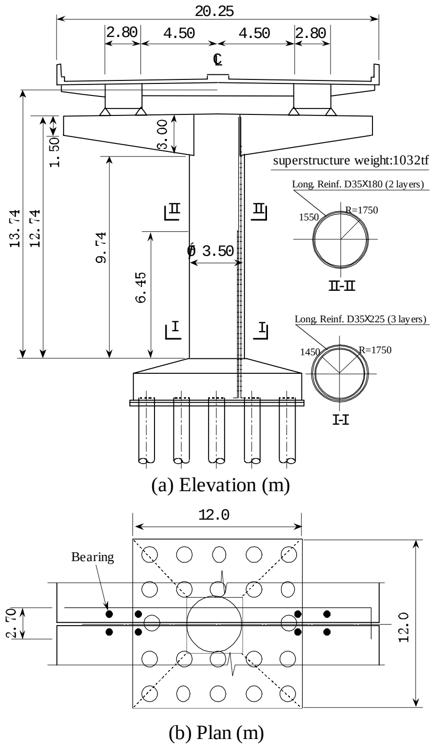

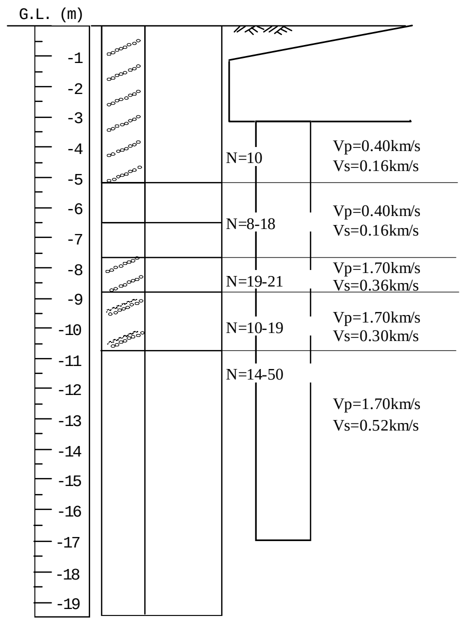

Figure 1: Bridge elevation and plan

Figure 2: Pile foundation and soil conditions

Analysis Approach

The sub-structure analysis method was used in the study (JSCE, 1989). The simulation system consists of two sub-structure systems: the under structure system and the upper structure system. The former includes foundations and foundation soils, and the latter includes the bridge superstructure, the pier and the soil spring calculated from the former.

The analysis flow is shown in Fig.3. First, an inverse analysis using the program SHAKE, was used to estimate the ground motion at the base-ground-surface from the ground motion wave recorded at the Japan Meteorology Agency in Kobe during the Hyogoken Nanbu Earthquake (Fig.4). The obtained base-ground-surface motion was assumed to be the same as that at the site of the bridge under investigation. SHAKE was then used again to calculate the response of the site ground (without any piles) under the excitation of the base-ground-surface motion. Thus, the equialent stiffness and the equivalent damping for each soil layer were obtained. These equivalent soil properties were used later for the under structure system (pile foundation and soil) analysis to obtain the effective input ground motion at the center of the footing for the simulation of the upper structure system (superstructure, pier with soil spring). The calculations obtained by SHAKE are based on a uniaxial response of layered soil by an equivalent linear method.

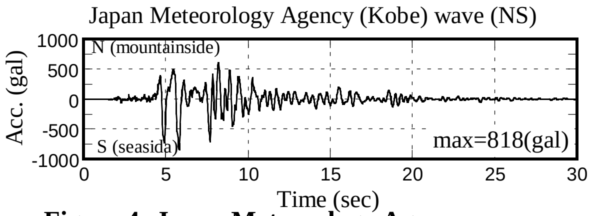

Figure 4: Japan Meteorology Agency wave

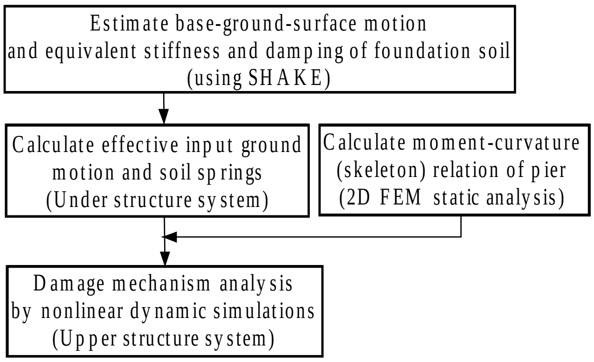

Figure 3: Analysis approach flow

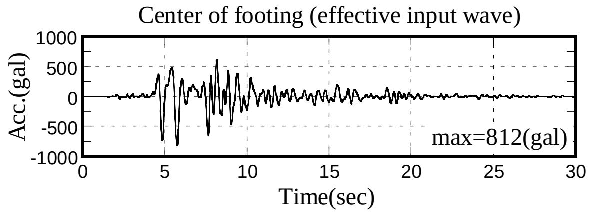

Figure 5: Effective input ground motion

Next, a three dimensional FEM analysis was carried out on the under structure system to investigate the response of the pile groups. This analysis took into account the effect of the ??geomatic?? interaction of the foundation soil and the piles. In this analysis model, only the foundation stiffness was taken into account while its mass was assumed to be zero. The effective input ground motion at the center of the footing and the equivalent soil springs as well as the equivalent soil damper were available (refer to Section 2.3).

Finally, the upper structure system was represented by a lumped-mass model, taking into account the nonlinear properties of the pier. The pier-foundation interaction was represented by the springs and dampers used in the previous step. The input wave at the pier bottom was the effective input ground motion. The effective factors were investigated using this simulation model.

In addition to the damping from the soil damper, 5% Rayleigh damping was added for the whole structure. The Newmark-β method was adopted with a time interval of 0.01sec and 10 iterations for each time step.

Effective Input Ground Motion and Soil Springs

The simulation results of the under structure system have been reported in detail by Sun (1998). The maximum acceleration of the base-ground-surface motion is 606gal, causing a maximum acceleration response of 812gal at the center of the footing (Fig.5). The uncoupled soil springs act at the center of the footing, 1.1m below the pier bottom. The values of the spring stiffness and the damper's damping are:

Horizontal direction: stiffness=1.75X10^5tf/m; damping=15%

Rotational direction: stiffness=1.42X10^6tf-m/rad; damping 5%

Vertical direction: not considered in this study

Basic Model of Upper Structure System for Analysis

The upper structure system was expressed by a lumped-mass model as shown in Fig.6. The footing region and the horizontal beam region above the pier top were modelled by rigid beam elements, and the pier region was modeled by nonlinear beam elements. This model assumes that the curvature in each pier element has a linear distribution, and the moment-curvature relations, i.e., skeleton curves, are set according to a static nonlinear FEM analysis (Ohuchi, 1997). The Takeda trilinear hysteresis rule was used for flexure, while the shear force-deformation is assumed to be inelastic. Here, considering that the bond length of reinforcement bars is 90cm, the reinforcement terminated height for the model is 5.5m (=6.4m-0.9m) above the pier bottom.

The bearing model comprised a total of 8 bearings for the bridge prototype. The girders of adjacent spans are assumed to have the same response, so the 8 bearings were modelled by 4 pairs of springs in the horizontal direction and vertical directions. The stiffnesses of the bearing springs were estimated from the stiffness of the side block for the horizontal direction and the compression stiffness of the bearing plate for the vertical direction.

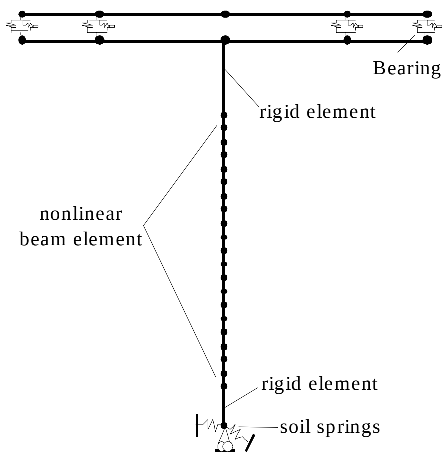

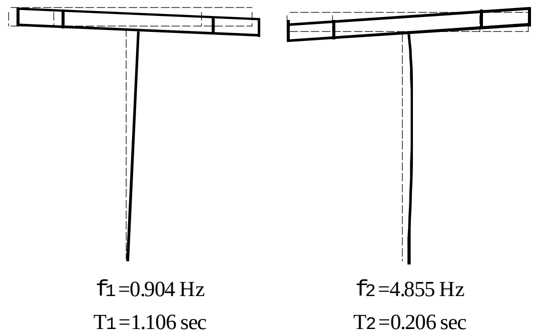

Figure 6: Simulation model for upper structure **Figure 7: Natural frequencies and modes**

MODELING FOR EFFECTIVE FACTORS

In this study, the effective factors determining the extent of bridge damage were investigated using different structural models. Each model was modified on the basis of the basic mode described in Section 2.4. These effective factors and their models are listed in Table.1.

Cracks at Pile Top

According to the field-investigation after the Hyogoken Nanbu Earthquake, cracks were detected in the joint region of RC piles and footings. To assess the effect of cracks in the pile tops, hinge connections were assumed instead of rigid connections between the piles and the footing. As a result, the simulation showed that there was almost no change for the rotational soil spring, but about a 25% reduction in the stiffness of the horizontal soil spring. Therefore, for the simulation of the upper structure system, the stiffness of the horizontal spring was reduced to 75% if the cracks in the joint region of the pile and footing were considered. However, experimental results of a real pile foundation (Sakamoto, 1998) with dimensions comparable to those of the bridge under investigation and was loaded by a horizontal force, showed that the skeleton curve of the nonlinear horizontal soil spring was as shown in Table 1. The model was set to have an origin-oriented hysteresis property.

Height of Terminated Longitudinal Reinforcement

For the basic model, the height of the terminated longitudinal reinforcement is 5.5m from the pier bottom. Damage investigations have reported that many bridge pier failures are due to premature termination of longitudinal reinforcement. In order to investigate this effect, the height of terminated longitudinal reinforcement was assumed to be reduced by 3.0m, i.e., 2.5m from the pier bottom.

Embeded Depth Near Pier Bottom

In Japan, ordinary roads on the ground usually go under viaducts in urban areas. In these cases, bridge piers of viaducts are embedded in the pavement layer of the ordinary road. In this study, the effect of embedding was investigated by assuming that the embedding layer consists of a 1.0m thick soil with an N-value of 15 with a 0.5m pavement above it.

The stiffness coefficients of the soil spring are assumed to be 1929kgf/cm^3 (1/10 of the value for concrete) for the pavement layer and 7kgf/cm^3 for the soil layer, with an N-value of 15. The pavement strength was assumed to be f'_{ck}=180kgf/cm^2, and the uniaxial compression strength of the soil was assumed to be 10kgf/cm^2. Bilinear slip spring models were used to express the soil springs, and their values were set accordingly.

Bearing

For a bearing model, a combination of a horizontal nonlinear spring and a vertical linear spring were used. The nonlinear horizontal spring was assumed to have a failure strength calculated by the following formula (JRA, 1991):
(weight supported (1032/4)) X (design seismic coefficient (0.2)) X (safety factor (1.7)) = 87.7tf.

Table 1: Modeling for effect factors

Effe. Factors	Basic Model	Model for Effective Factor
(1) Crack of pile	Soil spring = linear 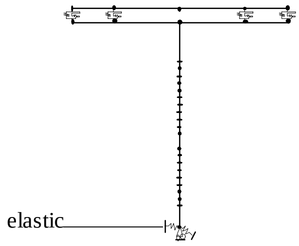	Soil spring = nonlinear 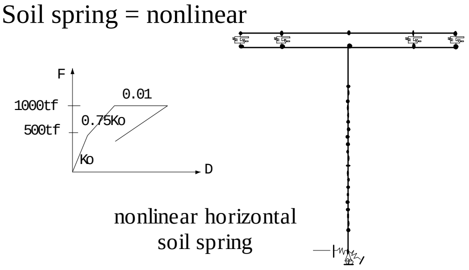
(2) Height of Term. reinf.	Height of termination = 5.5m 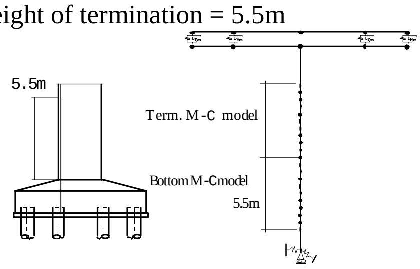	Height of termination = 2.5m 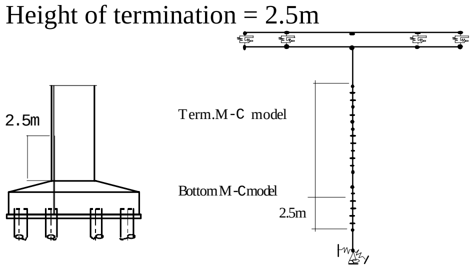
(3) Embedment	Depth of embedment = 0m 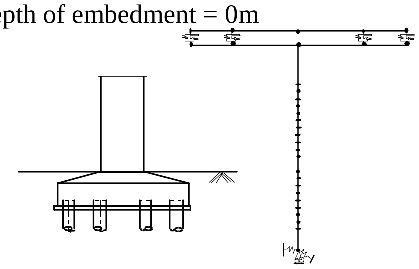	Depth of embedment = 1.5m 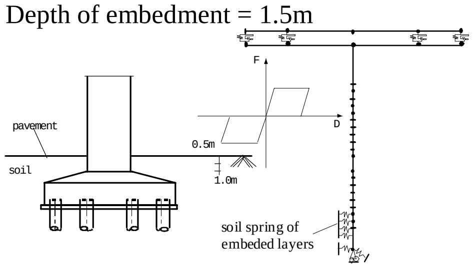
(4) Bearing	Bearing spring (horizontal) = elastic 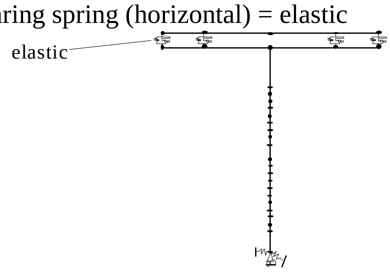	Bearing spring (horizontal) = bilinear 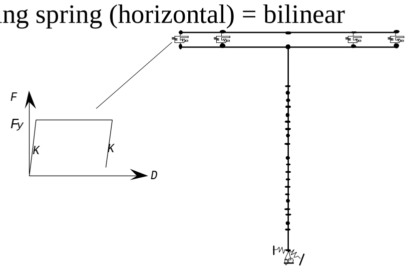
(5) Eccentricity	Eccentricity = 0m 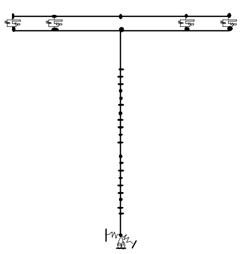	Eccentricity = +1.2m and –1.2m 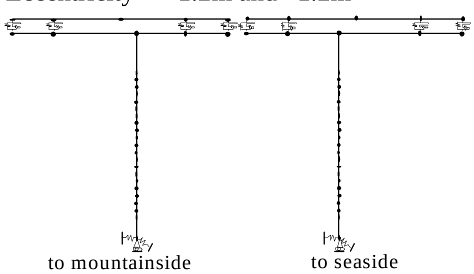

The behaviour of the bearing after failure is very complicated. At this moment, both theoretical and experimental research is lacking. Therefore, it is assumed that the bearing’s response after failure can be expressed by a sliding model with a friction coefficient between concrete-steel from 0.3 to 0.4. For the bridge investigated in this study, this friction force is coincidentally almost the same as the failure strength of the bearing. As a result, a bilinear friction type hysteresis model was adopted.

Superstructure Eccentricity

Simulations were also carried out assuming that a horizontal beam on the pier top and the superstructure has an eccentricity of 1.2m to the mountainside or seaside (Fig.4).

SIMULATION RESULTS

Natural Frequencies and Modes

As shown in Fig.7, the fundamental frequency for the basic model is 0.904Hz (1.106sec), and that of the second is 4.855Hz (0.206Sec). From the mode shapes, it can be determined that the first mode is due to the deformation of the bridge pier and the second is mainly due to the deformation of the soil springs. The input wave recorded at Japan Meteorology Angency in Kobe 1995 has a primary peak around 1.0sec, and this may be conjectured to cause a strong response of the bridge pier.

Earthquake Response Results

Simulations were carried out for 6 cases including the basic model and other models with modifications to the individual effective factors. The maximum results are shown in Table 2. The response time histories, hysteresis loops, are shown in Figs.8-10.

Table 2: Maximum results of dynamic analysis

Criterion for estimation		Case No.					
		1	2	3	4	5	6
		basic model	crack of pile	term. reinf.	embeded	bearing	eccenticity
pier bottom	shear (tf)	925	889	917	1180(1050*	899	951
	mom.(tf-m)	11800	11800	11800	11600(11700*)	11800	11900
	curv.(1/m)	4.23e-3	5.00e-3	3.57e-3	2.48e-3	3.26e-3	8.00e-3
	ductility	2.82	3.33	2.38	1.65	2.17	5.33
position of term. reinf.	shear(tf)	899	889	903	900	858	905
	mom.(tf-m)	9110	8780	10100	8730	8880	9930
	curv.(1/m)	1.09e-3	1.02e-3	3.20e-3	1.01e-3	1.04e-3	1.29e-3
	ductility	-	-	2.46	-	-	-
pier top	dis.(cm)	25.7	30.2	25.7	22.8	24.3	31.7
	vel.(kine)	169	170	166	155	166	157
	acc.(gal)	646	637	640	680	699	642
	resi.dis.(cm)	1.7	2.7	1.7	1.5	1.5	10.5
bearing	hori.force(tf)	159.8	158.3	156.9	164.3	88.0	154.6
	deform.(cm)	0	0	0	0	2.6	0
footing	hori.dis(cm)	0.8	7.4	0.8	0.8	0.8	0.8
soil spring	hori.force(tf)	1378	1118	1388	1115	1344	1471
	rot.M(tf-m)	14343	14586	14138	11715	13939	14790

*Value at the level of ground surface.

Basic model (case 1)

The maximum horizontal displacement at the pier top is 25.7cm, and the acceleration is 646gal. The section of terminated longitudinal reinforcement did not yield, while the section of the pier bottom yielded and the ductility ratio of curvature is 2.82. Thus, there is 1.7cm residual displacement (Fig.8). The reaction of the horizontal soil spring is 1378tf, which is larger then the value for yield of piles considered in case 2. The maximum displacement of the footing is 0.8cm.

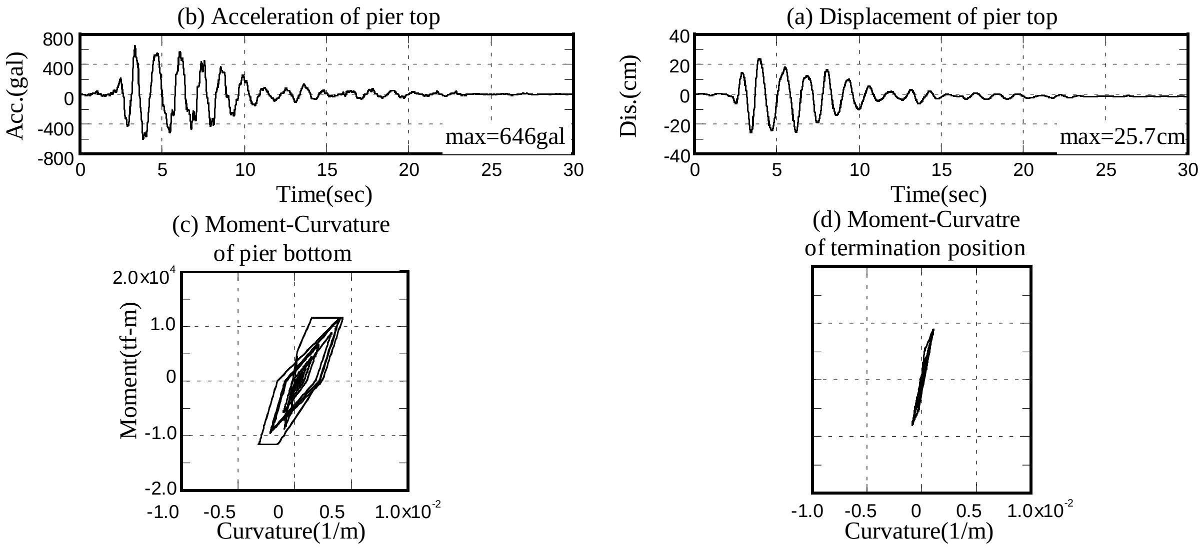

Figure 8: Response results (case 1)

Effect of cracks in pile-footing joint region (case 2)

Due to pile yielding, the footing has 7.4cm horizontal displacement. As a result, the maximum displacement for the pier top reaches 30.2cm. However, the maximum acceleration and the base shear force become slightly smaller than for case1.

Effect of height of terminated longitudinal reinforcement (case 3)

The terminated section yielded because of the lowered termination height of the longitudinal reinforcement. The maximum displacement of the pier top does not change much compared with the basic model (case 1), while the curvature distribution along the pier is changed.

Effect of embedded depth near pier bottom (case 4)

When considering a 1.5m depth from the pier bottom embedded in the soil and the pavement, the maximum curvature of the bottom section of the pier, the moment at the termination section and the reaction force of the soil spring at the footing become smaller. However, the maximum shear force in the pier increases by 20%, so a shear failure is likely in the section embedded in the ground surface. The reaction force-deformation of the soil springs for the embedded layers are shown in Fig.9.

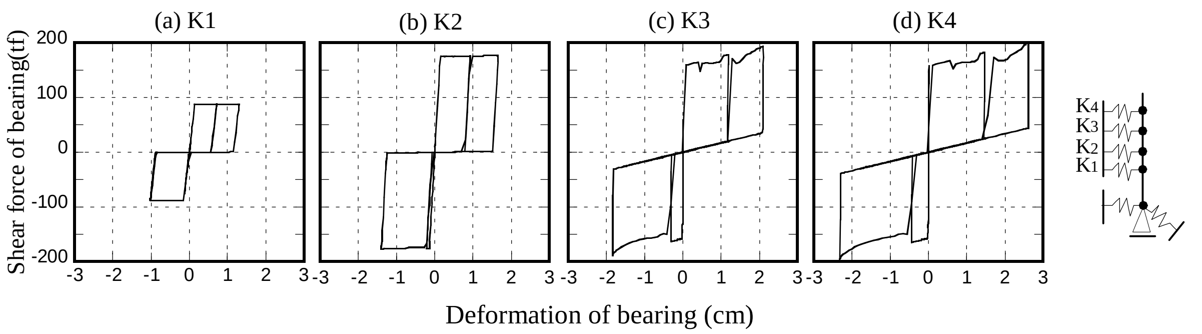

Figure 9: Responses results (case 4)

Effect of bearings (case 5)

The maximum displacement at the pier top and the maximum shear force at the pier are reduced due to bearing failure. Sun (1997) has reported that those reductions increase when the strength of the bearings becomes low. The stiffness of the bearing suddenly becomes zero when it fails. This causes an impulse-type acceleration incresease of the pier. Even though the section of pier bottom yields just as in the basic model, the maximum curvature reduces due to the bearing failure.

Effect of superstructure eccentricity (case 6)

The simulations with superstructure eccentricity to the mountainside or the seaside showed that the former, i.e., having eccentricity to mountainside, is an unfavorable situation, yielding a maximum displacement of 31.7cm at the pier top. Furthermore, the residual displacement increased to 10.5cm. This indicates that eccentricity promotes the development of damage after pier yield.

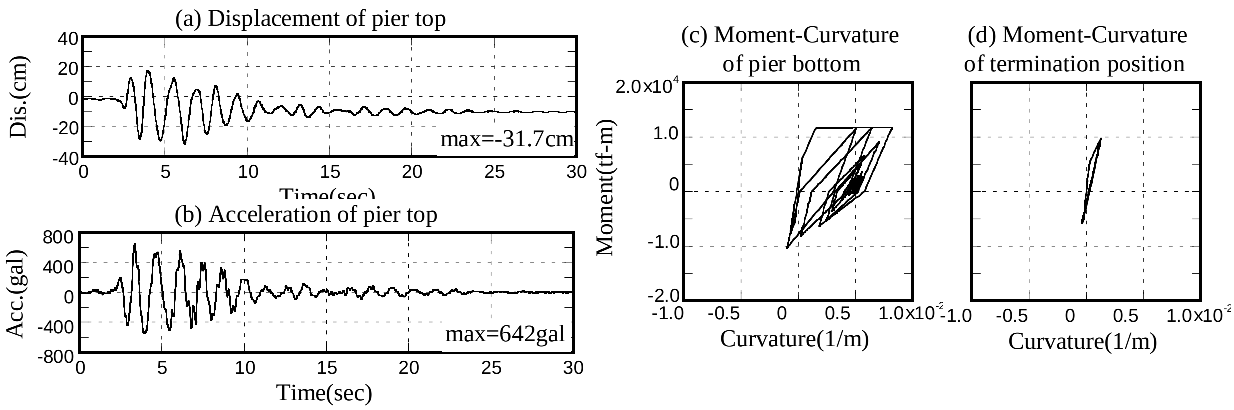

Figure 10: Responses results (case 6)

CONCLUDING REMARKS

The effects of several factors have been illustrated based on nonlinear dynamic simulations. The investigated factors were: (1) height of terminated longitudinal reinforcement; (2) stiffness of equivalent soil springs, representing damage to piles and nonlinear properties of foundation soil; (3) embedded depth of bridge pier; (4) failure of bearings; (5) eccentricity of superstructure.

The simulation results showed that: (1) the height of terminated longitudinal reinforcement is a major factor affecting the strength of the bridge pier. (2) damage to piles and eccentricity of superstructure result in a larger residual displacement. (3) the effect of embedded depth near bridge bottom should be taken into account in design, especially when the pier is embedded in the pavement. (4) failure of bearing may somewhat reduce shear force acting on the bridge pier.

REFERENCES

JRA (1991), *Manual of Bearings for Road Bridges,* Maruzen, Tokyo. (In Japanese)

JRA (Japan Road Association) (1996), *Design Specifications of Highway Bridges, Prat V. Seismic Design.*

JSCE (1989), *Dynamic Analysis and Seismic Design, Vol.2 Dynamic Analysis Method,* Gihoudo, Tokyo. (In Japanese)

JSCE (Japan Society of Civil Engineers) (1996), "Damage of Civil Engineering Structure, -Bridge-", *Hanshin-Awaji Earthquake Report,* Maruzen, Tokyo. (In Japanese)

Ohuchi, H., Hayashi, H., Kosa, K. and Tasaka, M. (1997), Collaps mechanism analysis of a RC bridge by using numerical simulation, *Proceedings of Annul Meeting of Japan Concrete Institute.* (In Japanese)

Priestley, M. J. N., Seible, F. and Calvi, G. M. (1996), *Seismic Design and Retrofit of Bridges,* John Wiley & Sons, New York.

Sakamoto, M., Hayashi, H., Morita, Y., Kasao, M. and Tomonaga, N. (1998), "Horizontal loading experiment of a 9 piles foundation", *Proceedings of 29th Japan National Conference on Soil Mechanics and Foundation Engineering,* pp1593-1598. (In Japanese)

Sun, L. M., Hayashi, H., Kosa, K., Goto, Y. and Ohuchi, H. (1997), "Research on relation between damage of bridge pier and failure of bearing", *Proceedings of 52nd JSCE Annul Meeting,* I-B, p722-723. (In Japanese)

Sun, L. M., Hayashi, H., Kosa, K., Goto, Y. and Ohuchi, H. (1998), "Nonlinear dynamic analysis of RC bridge pier damaged in Kobe earthquake", *Journal of Structure Engineering, JSCE,* Vol44A, p679-688. (In Japanese)